
Article:
Hu, Y., Watson, M., Maiorino, M. et al. (8 more authors) (2021) Experimental study on wear properties of wheel and rail materials with different hardness values. Wear, 477. 203831. ISSN 0043-1648

https://doi.org/10.1016/j.wear.2021.203831

Experimental study on wear properties of wheel and rail materials with different hardness values

Y. Hu[a,b], M. Watson[b], M. Maiorino[c], L. Zhou[a], W.J. Wang[a,], H. H. Ding[a*], R. Lewis[b], E. Meli[c], A. Rindi[c], Q.Y. Liu[a], J. Guo[a]

[a] *Tribology Research Institute, State Key Laboratory of Traction Power, Southwest Jiaotong University, Chengdu 610031, China*

[b] *Department of Mechanical Engineering, The University of Sheffield, Mappin Street, Sheffield S1 3JD,UK*

[c] *Department of Industrial Engineering, University of Florence, Via S. Marta 3, 50139 Firenze, Italy*

Abstract: This paper aimed to investigate the wear properties of different wheel-rail material pairs with various hardness values. Twin-disc wear experiments were carried out via cross-matching five types of wheel material (ER7, ER8, CL60, C-class and D-class) and four types of rail material (U71Mn, U75V, PG4 and PG5). The effects of bulk hardness, post-test hardness, hardening ratio, and rail/wheel hardness ratio (H_R/H_W) on the wear rate of wheel and rail materials were analyzed.

The results indicated that the wheel wear rates decreased with wheel bulk hardness and slightly increased with the rail bulk hardness. However, the rail wear rates decreased with the increasing wheel bulk hardness under 1% creepage and 1500 MPa contact pressure. In addition, both the wheel and rail wear rates showed increasing trends with the increase in wheel hardening ratio and the pre-test H_R/H_W. The surface damage of the harder C-class and D-class wheels, and the high-hardness PG4 and PG5 rail materials were relatively slight. The premium PG4 and PG5 rails possessed significantly shorter cracks than the base materials (ER8-U71Mn), whereas, U75V was relatively longer. The results will not only help optimize wheel and rail hardness matching, but also improve the prediction of wear and crack growth reliant on wheel and rail

* Corresponding author. Tel: +86-28-87634304.

E-mail address: haohao.ding@swjtu.cn (H.H. Ding).

material properties.

Keywords: Wear properties; Fatigue crack; Hardness; Rail/wheel hardness ratio

1. Introduction

The strategic matching of wheel and rail materials plays a key role in improving the asset life and reducing maintenance cost. In order to satisfy the demands of economy and safety, higher-quality wheel and rail materials have been developed to reduce wear degradation [1]. This makes the matching behaviour between wheel and rail complicated in current railway networks. However, no common regulations and standards have been proposed so far for the matching performance of wheel and rail steels. Therefore, it is necessary to carry out research on matching behaviour for wheel-rail pairs based on wear properties to provide a theoretical basis and technical support for optimal selection of wheel and rail materials.

Different grades of wheel and rail materials usually yield different bulk hardness values. The bulk hardness of wheel and rail steels commonly used in various countries are currently between 200 HB and 440 HB [2]. Bulk hardness has long been regarded as one of the most important material properties affecting wear, and its impact on wear properties has been extensively studied. These studies generally kept the rail or wheel material (but mainly the wheel) constant and changed the hardness of the counter body, and other parameters such as contact pressure and creepage in the contact were rarely varied. It was generally found that the wear rate of wheel and rail reduced with their increasing bulk hardness [3-15]. Some authors have settled on particular trends for the variation in wear rate as the hardness of counter body is varied, however, work has emerged that contradicts these trends. At first, it was believed that

an increase in the rail bulk hardness would give an increase in wheel wear loss [3-7], whilst increasing wheel bulk hardness could increase rail wear [8-10]. Whereas, recent studies [11-13] suggested that the wheel wear loss was independent of rail hardness. Furthermore, some studies [14,15] even found a result totally contrary to expectations, that is, the harder rail steel was beneficial to the matched wheel steel while enhancing its own wear resistance.

Rail/wheel material hardness ratio (H_R/H_W) is another important index to characterize the matching behaviour of different wheel-rail pairs. The relationship between H_R/H_W and wear loss, proposed by Steele & Reiff [16], indicated that with a consistent wheel material, the wear response of wheel and rail partly depended on the H_R/H_W value:

- When using a softer rail ($H_R/H_W \leq 1$), as the rail hardness increased, rail wear decreased whilst the wheel wear increased linearly;
- When the rail was harder than the wheel ($H_R/H_W > 1$), with an increase in rail hardness, the rail wear would continue to reduce, while the wheel wear would remain stable;
- The total wear decreased with the increasing H_R/H_W for both cases.

Furthermore, during cyclic loading, the contact surface of wheel and rail underwent work hardening induced by plastic deformation, prompting a significantly higher post-test surface hardness [17-19]. In actual wheel-rail contacts, the wheel and rail operate for most of the time at a steady state condition at run-in hardness. Consequently, the post-test hardness and work hardening levels for wheel and rail materials could have the largest influence on the wear properties. Some studies believed that a low work hardening level was the main reason causing the high wear of bainitic steel [20-22]. A study found that under 10% creepage and 1500 MPa pressure, the R350HT rail showed a substantially higher wear rate than two undefined premium

rail materials whose hardness was close to R350HT, at the start (1000 cycles). As the test passes increased to 10,000 cycles, the wear rates of the three rail steels were reduced to a similar value [23]. This may result from the fast work hardening of the premium materials.

In summary, in order to optimize the selection of wheel and rail materials, it is necessary to have a better understanding of the impacts of bulk hardness, H_R/H_W, post-test hardness and hardening level on wear responses. With the introduction of new premium wheels and rails as well as changing wheel/rail contact conditions, relationships defined, sometimes decades ago, need to be revisited and, through more parametric studies, new understanding and mechanisms need to be explored. Consequently, in this work, twin-disc wear experiments were carried out by cross-matching five types of wheel material (ER7, ER8, CL60, C-class and D-class) and four types of rail material (U71Mn, U75V, PG4 and PG5). The wear properties of the 20 wheel-rail pairs with various hardness values were investigated. The effects of bulk hardness, hardening ratio, pre-test and post-test H_R/H_W on the wear rate of wheel and rail materials were analyzed.

2. Experimental procedure

2.1 Material and processing

In order to learn more about the wear properties of various wheel and rail materials through experiments, five types of wheel steel (three standard wheel steels: ER7, ER8 and CL60; two premium steels: C-class and D-class) and four types of rail steel (two standard Chinese rail steels: U71Mn and U75V; two new premium steels: PG4 and PG5) were used in this study, even though some of them possess similar chemical compositions and mechanical properties.

Table 1 shows their chemical compositions. The five wheel materials are hypoeutectoid steels with a carbon content of less than 0.77 *wt%*, and consisting of proeutectoid ferrite and lamellar pearlite [24]. The four rail steels show pearlite microstructure, which consists of alternating ferrite and cementite lamella [25].With the increase in the carbon content, the bulk hardness values of wheel and rail materials increase, whilst the proportion of proeutectoid ferrite in wheel steels decreases. The average pearlite lamellar spacing (*Sp*) was measured by the circular line method [26]. The *Sp* values for ER8, ER7, CL60, C-class and D-class wheel steels are 129.3±29 nm, 126.1±32 nm, 104.7±21 nm, 96.8±28 nm and 89.1±10 nm, respectively, and the *Sp* values for U71Mn, U75V, PG4 and PG5 rail steels are 238.4±51 nm, 202.4±49 nm, 112.4±34 nm and 98.9±28 nm, respectively.

Table 1: Chemical compositions and mechanical properties of wheel and rail discs.

Comp-onent	Grade	Chemical composition (*wt*%)							Bulk hardness /$HV_{0.5}$	Rm/MPa	Elongat-ion/%
		C	Si	Mn	P	S	Cr	V			
Wheel	ER7	0.50	0.33	0.77	0.006	0.010	0.177	0.029	265±6	820-940	≥14
	ER8	0.54	0.33	0.75	0.005	0.007	0.177	0.029	254±7	860-980	≥13
	CL60	0.61	0.29	0.74	0.006	0.009	0.143	\	298±11	≥910	≥10
	C-class	0.69	0.76	0.76	0.007	0.008	0.028	0.029	354±10	\	\
	D-class	0.72	0.83	0.80	0.007	0.011	0.198	0.078	365±9	\	\
Rail	U71Mn	0.65-0.75	0.15-0.58	0.70-1.20	≤0.025	≤0.025	\	\	278±12	≥880	≥10
	U75V	0.71-0.80	0.50-0.70	0.75-1.05	≤0.025	≤0.025	\	\	303±14	≥980	≥10
	PG4	0.75~0.82	0.70~1.05	0.50~0.83	≤0.025	≤0.025	\	\	390±15	\	\
	PG5	0.90~0.95	0.48~0.52	0.94~1.02	0.01~0.014	0.04~0.07	\	\	405±17	\	\

In order to reduce the impact of sampling depth on hardness [27] and try to simulate the on-site contact condition, except for the ER8 wheel samples (because of the lack of new wheels, the sampling position of ER8 samples was about 20 mm deeper than other wheel samples), all samples were taken at the same depth of 5 mm below the wheel tread and the rail head. The hardness of ER8 is slightly lower than that of ER7 in this work (Table 1), while the hardness of

the ER8 tread in field is generally slightly higher than that of ER7. The diameter was 50 mm for both the wheel and rail samples, and the contact width was 5 mm, see Ref. [25] for more details of sampling position and detailed sizes.

2.2 Rolling-sliding experimental details

The experiments were performed under dry conditions using a twin-disc apparatus (MJP-30A, China) [28], which allows two discs to run against each other with controlled normal and tangential forces to simulate the rolling-sliding contact between wheel and rail. These two discs are driven by two independent electric motors. The required creepages can be achieved by adjusting the different rotational speeds of discs.

The twin-disc approach was proposed to be the best approach to study the wear of wheel and rail materials as it provides the most cost- and time-effective methodology and it provides close control of test parameters which leads to more reliable and usable data, even though it has some issues, such as temperature effect, dimensional effect, etc. [29]. Based on previous research experience [29], the wheel and rail discs were machined into flat surfaces (line contact) to avoid an increase in contact area during a test and a subsequent reduction in the contact pressure.

To simulate the on-site wheel-rail contact status, the maximum contact pressure at the contact interface of wheel-rail discs in twin-disc tests should be consistent with those of the on-site conditions. The maximum contact pressure $\sigma_{\max}$ (MPa) is calculated using the Hertzian line contact formula [29]:

$$\sigma_{\max} = \sqrt{\frac{F\left(\sum \rho\right)}{\pi \cdot L\left(\frac{1-\mu_1^2}{E_1} + \frac{1-\mu_2^2}{E_2}\right)}} \tag{1}$$

where σ_{max} is the maximum contact pressure (MPa), F is the moral force (N), μ_1 and μ_2 are the Poisson's ratios of wheel and rail, respectively, E_1 and E_2 are the elastic modulus (MPa) of wheel and rail, respectively, L is the contact width (mm) of wheel and rail discs, and $\Sigma\rho = 1/R_1+1/R_2$, where R_1 and R_2 are the disc radii (mm).

Twenty wheel-rail pairs with various H_R/H_W values were achieved via cross-matching ER7, ER8, CL60, C-class and D-class wheel discs with U71Mn, U75V, PG4 and PG5 rail discs. It should be pointed out that the experiments for C-class-U71Mn, C-class-U75V and C-class-PG5 pairs have been carried out in Ref. [25]. All tests were performed under the same conditions (contact pressure: 1500 MPa; creepage: 1%; rotational speed of rail discs: 500 rpm; rotational speed of wheel discs: 495 rpm). In order to achieve a stable wear state (previous studies [11,20,30] showed that it can be reached within 20000 cycles), the total number of cycles for all tests was set to 25000. The test parameters are listed in Table 2. Each set of tests was repeated twice. Experiments were strictly implemented in accordance with the proposed test approach by Lewis et al. [29].

Table 2: Summary of test conditions.

No.	Wheel	Rail	H_R/H_W	Pressure/MPa	Creepage/%	Speed/rpm	Cycles
1#	ER7	U71Mn	1.047	1500	1	500	25000
2#		U75V	1.143	1500	1	500	25000
3#		PG4	1.470	1500	1	500	25000
4#		PG5	1.530	1500	1	500	25000
5#	ER8	U71Mn	1.093	1500	1	500	25000
6#		U75V	1.192	1500	1	500	25000
7#		PG4	1.533	1500	1	500	25000
8#		PG5	1.597	1500	1	500	25000
9#	CL60	U71Mn	0.933	1500	1	500	25000
10#		U75V	1.018	1500	1	500	25000
11#		PG4	1.309	1500	1	500	25000
12#		PG5	1.363	1500	1	500	25000
13#	C-class	U71Mn [25]	0.783	1500	1	500	25000

14#		U75V [25]	0.854	1500	1	500	25000
15#		PG4	1.099	1500	1	500	25000
16#		PG5 [25]	1.144	1500	1	500	25000
17#	D-class	U71Mn	0.760	1500	1	500	25000
18#		U75V	0.830	1500	1	500	25000
19#		PG4	1.067	1500	1	500	25000
20#		PG5	1.111	1500	1	500	25000

The wear loss of wheel and rail discs, was measured by an electronic balance (JA4103, accuracy: ±0.0001g). The surface hardness and sub-surface hardness were measured using a Vickers hardness instrument (MVK-H21, Japan) with 4.9 N load ($HV_{0.5}$) and 0.49 N load ($HV_{0.05}$), respectively. Before and after each experiment, ten points were evenly taken in the circumferential direction of the wheel and rail discs for the surface hardness measurement. Sub-surface hardness tests were performed on the worn discs along the depth direction of the longitudinal section. The measurements were made at intervals of 50 μm, with a total depth of 700 μm, and three times for each depth. Three small pieces separated by 120° of about 1 mm length were taken from each disc. Each section piece was cut along the rolling direction and prepared for microstructure observation by standard metallographic procedures. More details about the sampling position for metallographic observations can be found in Ref. [25]. The worn surfaces and fatigue cracks were characterized by using optical microscopy (OLYMPUS BX60M, Japan) and SEM (JSM-7800FPRIME, Japan). The length and depth of each surface crack were measured using an OM equipped with an image analysis software.

3. Results

3.1 Wear rate

Fig. 1 shows the wear rates as a function of wheel and rail bulk hardness. The wear rates of ER7, CL60, C-class and D-class wheel discs decrease as the wheel bulk hardness increases,

and increase slightly as the bulk hardness of the matched rail steels increases. However, the wear rates of ER8 wheel discs are stable at around 80μg/m, hardly affected by the hardness of the matched rail discs, as shown in Fig. 1a,b. The total wear rates (Fig. 1e,f) show a reduction trend with the wheel bulk hardness. Curiously, the rail wear rates do not seem to robustly correlate with the rail bulk hardness, however, they decrease with the increasing hardness of the matched wheels, as shown in Fig. 1c,d.

Notably, in the wheel-rail pairs with harder C-class and D-class wheels, the wheel, rail and total wear rates are visibly lower than those in other wheel-rail pairs. This means that the high-hardness wheel steels not only contribute to reducing wheel wear, but also favour a simultaneous reduction in rail wear. This will be discussed later.

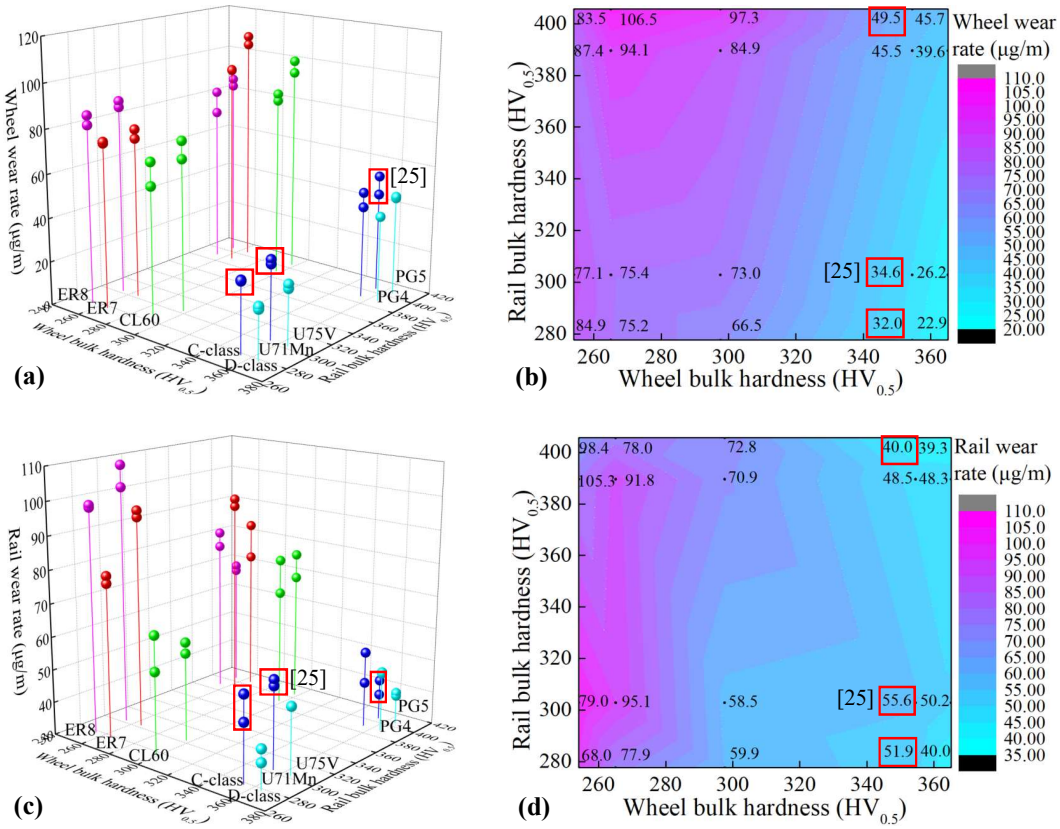

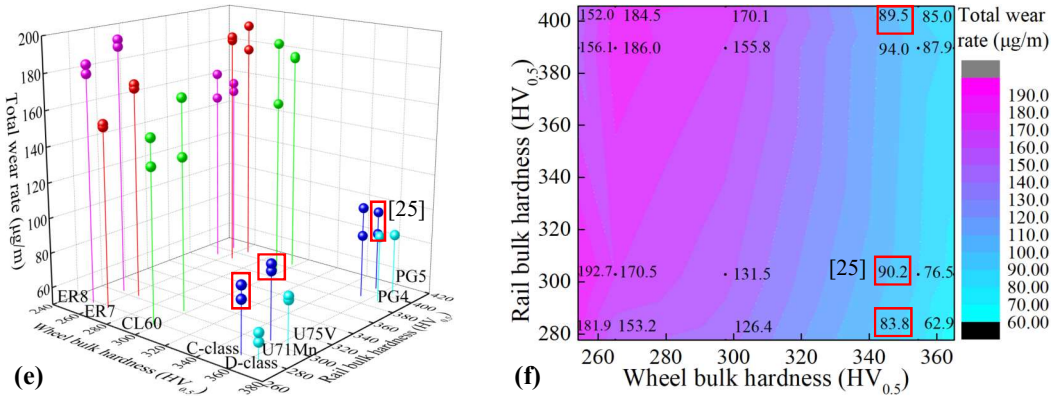

Fig. 1. Wear rate as a function of wheel and rail bulk hardness, (a) and (b) wheel; (c) and (d) rail; (e) and (f) total system. The data in the red box is cited from the previous work [25].

3.2 Hardness variation

Fig. 2 shows the pre-test and post-test surface hardness of wheel and rail discs. It is clear that the post-test surface hardness values are much higher than their bulk hardness for all discs. It means that the wheel and rail materials have undergone significant work hardening during the applied rolling-sliding cycles. The average post-test surface hardness values of wheel discs are in a range of around 770~870 $HV_{0.5}$, and those of rail discs are in the range of 700~900 $HV_{0.5}$.

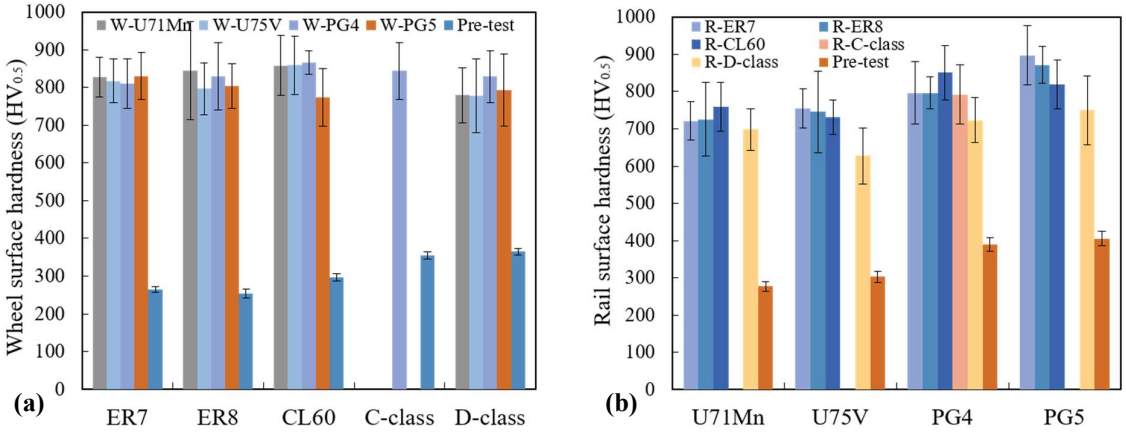

Fig. 2. Pre-test and post-test surface hardness, (a) wheel; (b) rail.

The variation of H_R/H_W is shown in Fig. 3a. The values of post-test H_R/H_W across all

experiments are similar and in a range of 0.8 ~ 1.2. The post-test H_R/H_W values for wheel-rail pairs with PG4 and PG5 rails are substantially smaller than their pre-test H_R/H_W values.

Fig. 4 shows the hardening ratio (*Hardening ratio* = $(H_{post}-H_{pre})/H_{pre}$, where H_{post} and H_{pre} are the pre-test and post-test surface hardness, respectively) of wheel and rail discs. It can be seen that the hardening ratio of the wheels and rails is related to their material properties, but independent of the matched material. The hardening ratio of wheel and rail materials shows a decreasing trend with an increase in bulk hardness.

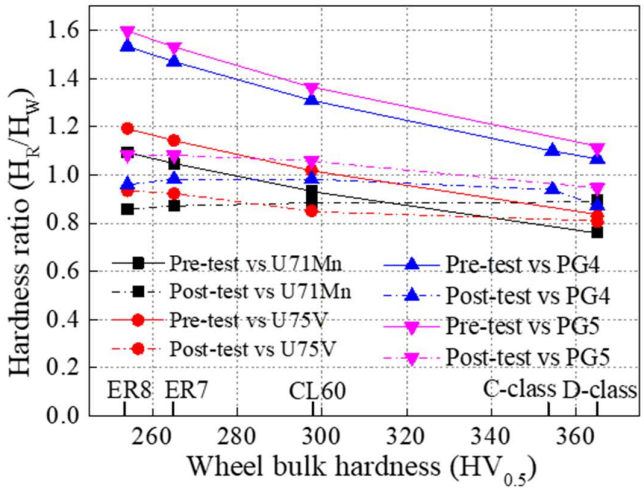

Fig. 3. Variation of hardness ratio (H_R/H_W).

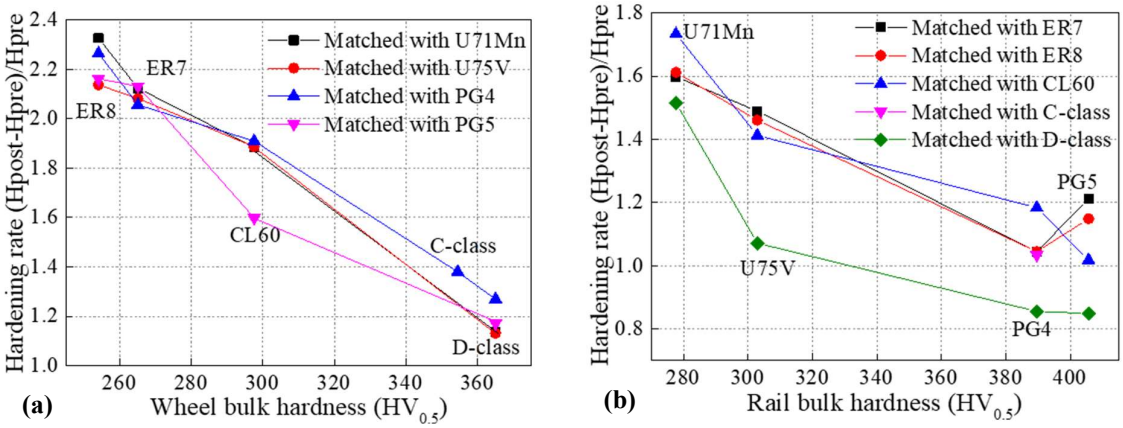

Fig. 4. Variation of hardening ratio, (a) wheel; (b) rail.

Fig. 5 shows the sub-surface hardness variation versus depth from surface for some

experiments. As the depth from the contact surface increases, the sub-surface hardness first drops sharply and then gradually stabilizes. It can be seen from Fig. 5a that in the severely hardened layer within 200μm from the surface, the sub-surface hardness of the premium C-class and D-class wheel discs is slightly lower than that of the ER7, ER8 and CL60 wheel discs. This may be related to the significantly lower hardening ratio of C-class and D-class wheel materials, as shown in Fig. 4a. When matched with different rail materials, no significant difference in the wheel sub-surface hardness distribution can be seen in Fig. 5b. Fig. 5c shows that the sub-surface hardness of premium PG4 and PG5 rails is slightly higher than the U71Mn and U75V rail discs at the same depth. Meanwhile, Fig. 5d shows similar sub-surface hardness variations of rail discs when matched with various wheel steels.

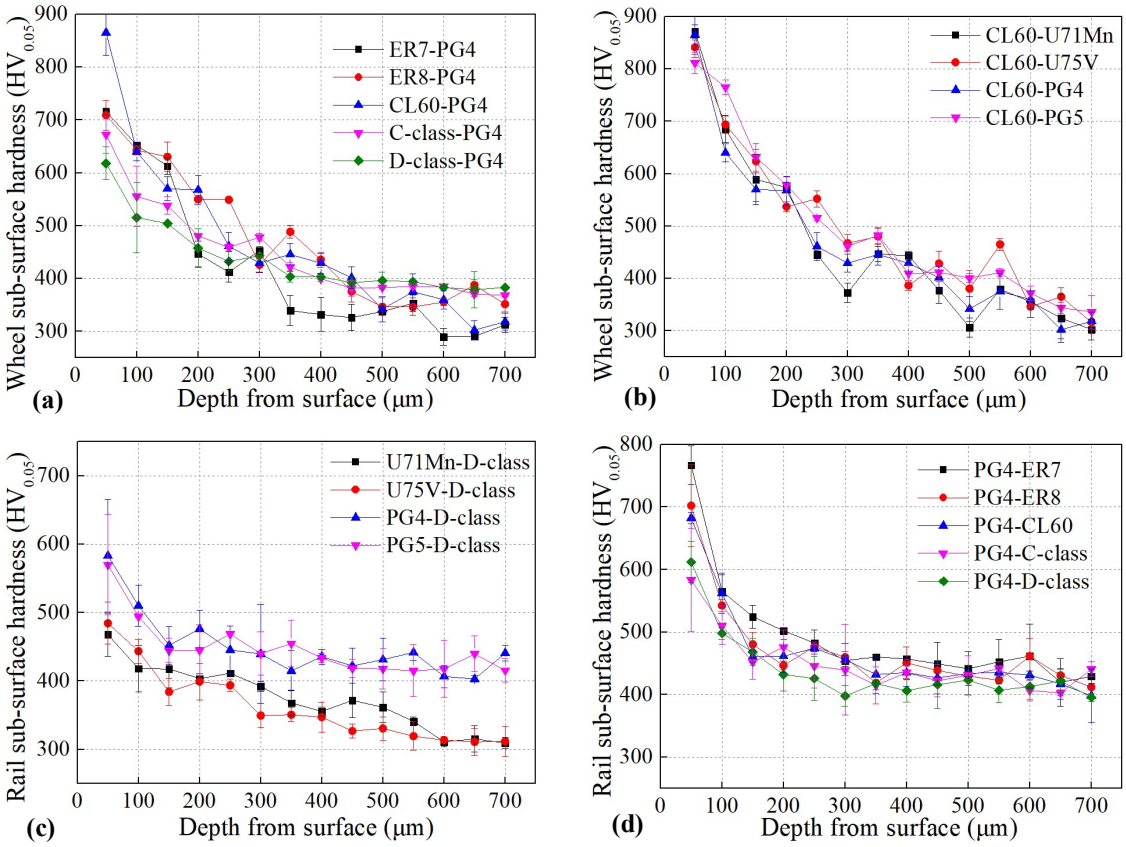

Fig. 5. Variation of sub-surface hardness versus depth from surface, (a) various wheel steels matched with

PG4 rail; (b) CL60 wheel matched with various rail steels; (c) various rail steels matched with D-class rail; (d) PG4 rail matched with various wheel steels.

3.3 Worn surfaces

The worn surfaces of wheel and rail discs are shown in Fig. 6. Due to the similar damage for each disc when matched with different materials, only a small sample of the observations are presented. The surface damage for the five wheel steels is generally typified by peeling (Fig. 6a-e). The surface damage for low-hardness ER7, ER8 and CL60 steels is severe, mainly by continuous peeling through the contact width (Fig. 6a-c), and the spacing between adjacent peelings is relatively large. In contrast, the premium C-class and D-class steels present mild peeling and smaller spacing, as shown in Fig. 6d,e.

Meanwhile, the surface damage for the four rail steels is dominated by ratcheting (the earlier stage of peeling) and mild peeling. Similarly, the more severe damage is observed in the softer U71Mn and U75V rails, shown in Fig. 6f-i. This evidence suggests that the surface damage reduces with the increasing bulk hardness.

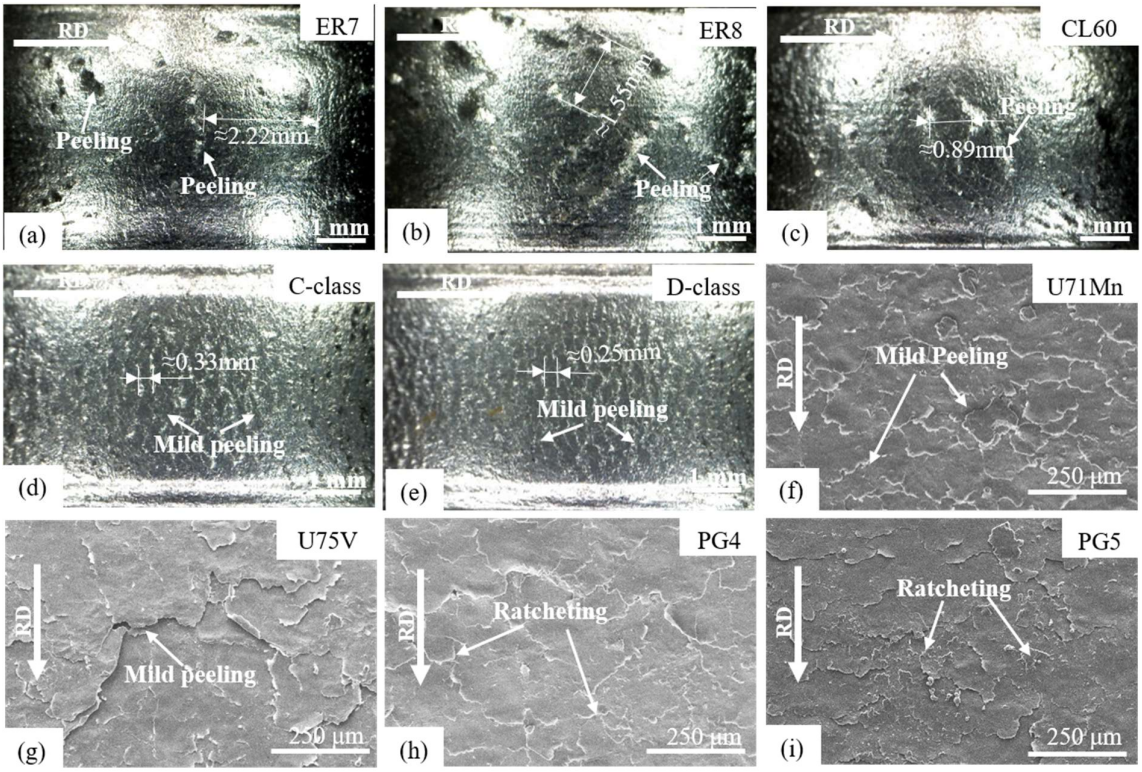

Fig. 6. Worn surfaces for wheel and rail discs, (a) ER7; (b) ER8; (c) CL60; (d) C-class; (e) D-class; (f) U71Mn; (g) U75V; (h) PG4; (i) PG5. The observed wheel discs were matched with PG4 rails, and the observed rail discs were matched with D-class wheels.

3.4 Fatigue cracks

The fatigue crack observations of wheel and rail steels are shown in Fig. 7. Numerous surface and sub-surface cracks can be seen on ER7 and D-class steels (Fig. 7a,b). The term "surface crack" refers to cracks that grow from the contact surface into the material, and the term "sub-surface crack" refers to cracks that have initiated in the sub-surface and have not yet propagated to the surface. When the sub-surface cracks further grow to the contact surface, they will form surface cracks. These surface cracks grow at a shallow angle (4.5° ~ 6.3° for ER7 and 7.2° ~ 7.8° for D-class). Similarly, the crack propagation for both soft U71Mn and hard PG4 rails is dominated by low-angle surface cracks (Fig. 7c,d). Branching and crack blunting,

occurring at the kink structures for rail materials, can be seen in Fig. 7c,d.

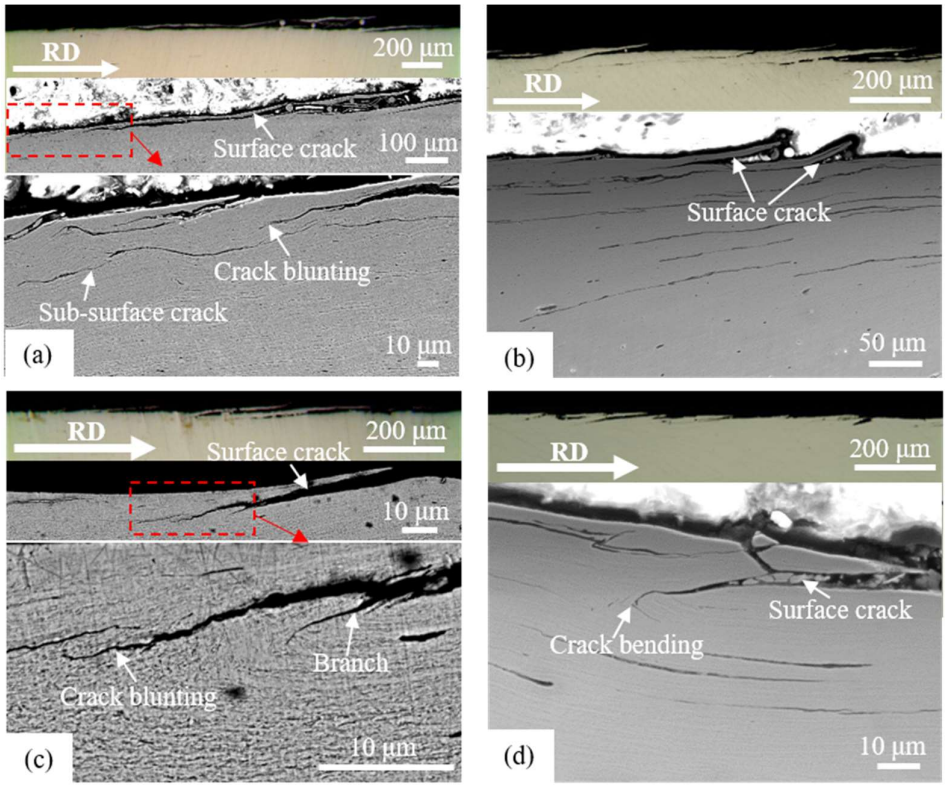

Fig. 7. Fatigue cracks of wheel and rail materials, (a) ER7 wheel; (b) D-class wheel; (c) U71Mn rail; (d) PG4 rail. The observed wheel discs were matched with PG4 rails, and the observed rail discs were matched with D-class wheels. The surface crack refers to the cracks that grow from the contact surface to the inside, and the sub-surface crack refers to the cracks that have initiated in the sub-surface and have not yet propagated to the surface.

Crack length data were analyzed by a generalized linear model (GLM) with gamma distributed error terms and an identity link function. The log of the crack length was the dependent variable. Explanatory, categorical variables for each material were added, as well as for each interaction of materials. Model terms were compared by T-tests to determine statistical significance. The assumption of gamma distributed errors was validated by inspection of Quantile-Quantile plots of the residuals. Besides, crack count data were analyzed by another

GLM with Poisson distributed error terms. The crack size data and QQ plots are given in Tables S1 and S2, and Fig. S1 of the supplementary material. The analysis results of crack data are presented in Fig. 8.

The ER8-U71Mn pair, which is most commonly used in Chinese high-speed railway, was taken as the base wheel-rail pair. The statistical analysis indicated that there was no significant difference in the length of wheel cracks, which were robust to adding interaction effects. Whereas, compared with the baseline pair (ER8-U71Mn), significantly more cracks were observed in C-class, D-class wheel materials, as well as the wheels matched with PG4 and PG5 rail steels.

The fatigue cracks in PG4, PG5 rails, and rails matched with D-class wheel material, were significantly shorter than those in the base materials, whereas, cracks in U75V were significantly longer. These were robust to adding interaction effects. The only significant interactions were PG4-CL60, PG5-C-class, PG5-CL60, PG5-D-class, PG5-ER7, which were all significantly shorter than the baseline. Furthermore, PG4, PG5 rails, and rails matched with ER7 and D-class wheel materials, possessed significantly more cracks than the baseline pair, while U75V had significantly fewer cracks than the baseline pair.

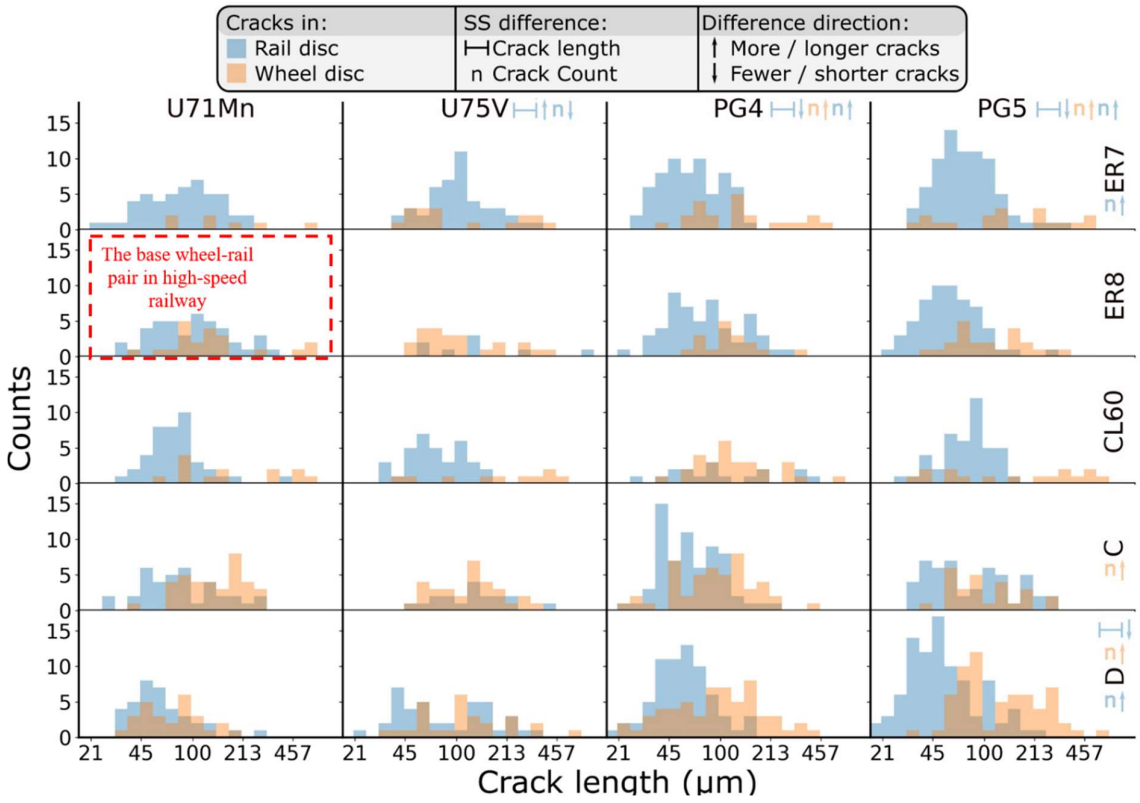

Fig. 8. Histogram grid of crack length. SS difference means statistically difference.

4. Discussion

4.1 Effect of bulk hardness on wear

The correlation between wear rates and hardness indexes (wheel and rail bulk hardness, post-test wheel and rail hardness, pre-test and post-test H_R/H_W) was analyzed by ordinary least squares regression models. Specifically, the model for the correlation between wear rates and wheel/rail bulk hardness is:

$$\text{Wear rate} = a_0+a_1*H_W+a_2*H_R+a_3*(H_R*H_W) \quad (2)$$

where H_W and H_R are the bulk hardness of wheel and rail, respectively, H_R*H_W is the interaction term, which can indicate the correlation between the influence of H_W or H_R on wear rate and H_R or H_W. Setting an interaction term can greatly improve the interpretation of the

dependence between variables in the regression model.

These statistical results indicated that:

- The wheel wear rate was significantly, negatively correlated with wheel bulk hardness, whilst significantly, positively correlated with rail bulk hardness;
- The rail wear rate was significantly, negatively correlated with wheel bulk hardness. Interestingly, this correlation was not robust to adding any interaction effects between wheel and rail hardness, so it is possible that this is really an interaction effect rather than a pure correlation (e.g. in reality it depends on H_R/H_W not purely H_W), but none of the simple interaction effects were significantly correlated either, this might be an interesting point for further work.
- The total wear rate was near significantly, negatively correlated with wheel bulk hardness; significantly, positively correlated with rail bulk hardness; and significantly, positively correlated with the interaction term (H_R*H_W).

The responses of wheel and total wear with bulk hardness were in agreement with previous studies [13,31], that is, the harder wheel/rail possesses better wear resistance but is slightly harmful to the counter body. However, the negative correlation between rail wear rates with the wheel bulk hardness, was contrary to the traditional expectation (introducing a harder disc will cause increased wear in the counter body) [32].

A similar phenomenon has also been found in other studies. For example, Santa *et al*. [33] compared the wheel and rail wear rates for E8 (260HV)-R400HT (435HV) pair with those from tests with other wheel and rail materials in previous studies, where the rails were all softer than R400HT. A lower wear rate was observed in both R400HT rail and the E8 wheel material for

all the $T\gamma/A$ values. The low wear rate for E8 wheel was caused by matching it with the hard R400HT. Heyder & Maeder [15] cross-matched the ER7, ER8 and C64M (high strength) wheel steels with R260, R350HT, R400HT and CrB1400 rail steels (R350HT and R400HT are pearlitic high-strength steels, CrB1400 is bainitic high-strength steel) in a full-scale study. It was found that the total wear rate was clearly lower for wheel-rail pairs with at least one high-strength material than that for the "standard" ER7-R260 pair.

These outcomes support the use of high-hardness rail in reducing both rail and wheel wears simultaneously. However, this study presents that harder wheel steels can give a simultaneous reduction in both wheel and rail wears, which contradicts with these previous results [15,33]. The potential reasons for this controversial wear response are: whether the wheel or rail is driving (which is faster, the rail or wheel) [11]; the third body layer (debris and roughness); test conditions and test cycles.

In this work, the rail disc was faster than the wheel disc, which means that the wheel was driven (simulating a braking wheel). In contrast, in the twin-disc tests of literature [15,33], the wheel disc was faster than the rail disc, simulating a traction wheel. This difference may have caused the converse wear response that a lower wheel wear rate was found with a higher rail hardness in literature [15,33], while a higher wheel hardness gave a lower rail wear rate in this work.

Besides, during rolling-sliding, debris was drawn into the contact interface and tended to adhered to the faster disc (driving disc), forming a third body layer, which would affect the action state of the contact pressure and the distribution of creepage in the interface, thereby influencing the wear state [34]. For example, Zhou *et al.* [35] found that the wheel and rail wear

rates at low temperature were significantly lower than those at room temperature because the faster disc was covered by a third body layer at low temperatures. In this work, although the third body layer was not formed, the surface damage and crack length of the faster rail discs (Fig. 6f-i, Fig. 8) were significantly lower than those of wheel discs (Fig. 6a-e, Fig. 8). This suggests that the debris still had an effect on the damage of the faster disc. This may also be a potential reason why the wear rate of the faster disc (rail) was less affected by the bulk hardness. As mentioned above, the surface damage of different wheels was quite different, which could cause different roughness in the contact interface [36]. Thereby, it could affect the rail wear.

Moreover, it is generally known that a transition of wear regime occurs in different test conditions (creepage and contact pressure, i.e., $T\gamma/A$). The wear response of different materials under different conditions was variable [11,37,38]. For example, in the literature [11] the wheel wear rate matched with the R350HT rail was higher than that matched with the R260 rail at 1% creepage. Whereas, the results were opposite at 10% and 20% creepage. Based on the above, a twin-disc experiment was performed for the ER7-U75V and C-class-U75V pairs under 3%, 1500 MPa. It was found that at 3% creepage, the wheel wear decreased and the rail wear increased with the increase in the wheel bulk hardness, which agreed with the general cognition [8-10]. On the contrary, at 1% creepage, the wear rates of both wheel and rail reduced with the increasing wheel hardness (Fig. 1a-d). This confirms the conjecture that the wear trend is related to test conditions. However, at 3% creepage, corrugation occurred on rail discs, which was also seen in other studies [10]. The occurrence of corrugation would have an impact on the wear response.

The short test cycles in this work would partially affect the judgment of wear trend.

Therefore, it is necessary to perform more closely monitoring for wear rate to confirm that steady state wear has been achieved.

4.2 Effect of pre-test H_R/H_W on wear

Fig. 9a-c shows the wear rates as a function of pre-test H_R/H_W. Overall, the wear rates of wheel, rail and total system increase with the increasing pre-test H_R/H_W value. However, in the overlapping area (H_R/H_W is in the range of 1.0 ~ 1.2, shown in the red box of Fig. 9a-c), wear rates for the wheel-rail pairs with C-class and D-class wheels are substantially lower than those for other wheel-rail pairs. This indicates that regardless of the pre-test H_R/H_W, the material properties still account for the main factors affecting the wear rate.

In the relationship between wear and H_R/H_W reported by Steele & Reiff [16], it was evidenced that the change of wheel wear with H_R/H_W was different around the H_R/H_W of 1, as shown in Fig. 9d. Based on that, a pre-test H_R/H_W slightly greater than 1, i.e. the rail was slightly harder than the wheel, was generally considered to be the most reasonable choice in the field. Razhkovskiy *et al*. [39] believed that the optimal pre-test H_R/H_W was 0.91 ~ 0.97 or close to 1. However, this work did not show a correlation with the pre-test H_R/H_W around 1 (the black dotted-lines in Fig. 9a-c).

Besides, in Fig. 9d with the constant wheel hardness, as the H_R/H_W increased (i.e., the rail hardness increased), the rail and total wear decreased, and the wheel wear increased first and then remained stable. In this study, when the wheels are constant (the same shape in Fig. 9a-c), the wheel and total wear rates increase with the increasing pre-test H_R/H_W. The rail wear rates matching the C-class and D-class wheels increase first and then decrease (the turning point occurs at the pre-test H_R/H_W of about 1), while the wear rates of rails matching ER7, ER8 and

CL60 wheels do not show similar trends because the pre-test H_R/H_W values are greater than 1.

When the rails remain constant (the same colour in Fig. 9a-c), the wear rates of wheel, rail and total system increase as the pre-test H_R/H_W increases. These trends are different with those in Fig. 9d. This may be related to the different materials used in the two studies, the set test parameters, and the test environment. Furthermore, Fig. 9d did not give specific wear data and H_R/H_W values. With the development of premium wheel and rail materials in recent years, it is not likely that the relationship in Fig. 9d still applies to the selection of wheel and rail materials in field.

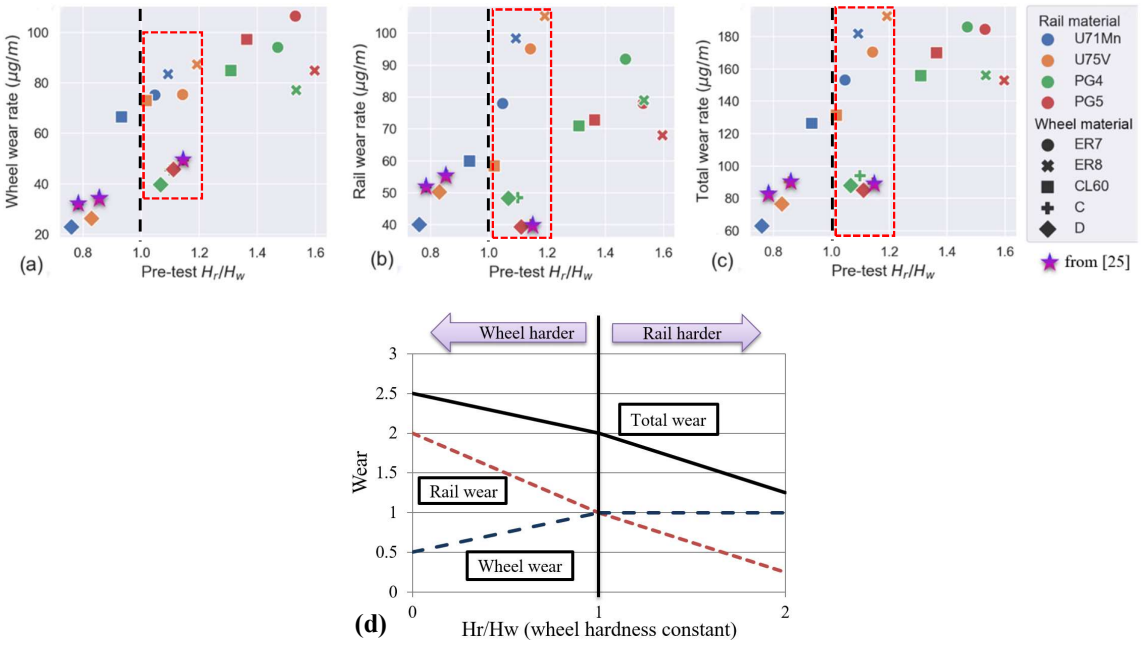

Fig. 9. (a-c) Wheel, rail, total wear rates as a function of pre-test H_R/H_W; (d) the relationship between wear and H_R/H_W reported by Steele & Reiff [16]. The overlapping areas of H_R/H_W are marked by red boxes.

4.3 Effect of post-test hardness indexes on wear

The statistical analysis for the wear rates versus post-test wheel/rail surface hardness (see the supplementary material, Fig. S2 and Fig. S3) indicated that there was no statistically significant correlation between the post-test hardness and the wear rates of wheel, rail and total

system.

However, materials with different bulk hardness presented similar post-test surface hardness (770 $HV_{0.5}$ ~ 870 $HV_{0.5}$ for wheels and 700 $HV_{0.5}$ ~ 900 $HV_{0.5}$ for rails, as shown in Fig. 2), proving the existence of different levels of work hardening, which may potentially affect wear responses. Wear rates as a function of wheel hardening ratios are given in Fig. 10. Apparently, the wear rates of wheel, rail and total system increase linearly with the increase in wheel hardening ratio.

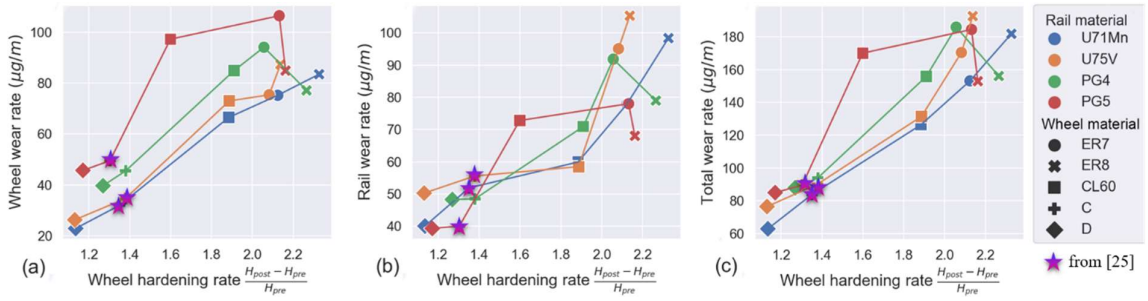

Fig. 10. Wear rates as a function of wheel hardening ratio: (a) wheel; (b) rail; (c) total system.

It was not found that the rail hardening ratio had a significant effect on wear response (see the supplementary material, Fig. S4). The post-test H_R/H_W was centralized in a small range of 0.8 ~ 1.2 (Fig. 3), which makes it hard to observe the effect of post-test H_R/H_W on the wear response (see the supplementary material, Fig. S5).

In summary, the bulk hardness and the hardening ratio of wheel and rail materials, as well as the H_R/H_W had important impacts on wear response. However, all results showed that the material properties are the main factor affecting wear properties. Therefore, the relationship between microstructure evolution of materials with different hardness and their hardening and wear properties needs to be further studied. In addition, although a wide range H_R/H_W of 0.7 ~ 1.6 was studied in this work, only one test condition (1500 MPa, 1%, 500 prm) was set.

Therefore, it is necessary to conduct hardness matching experiments under different parameters to improve the wear map based on H_R/H_W and $T\gamma/A$.

5. Conclusions

In this work, five types of wheel materials (ER7, ER8, CL60, C-class and D-class) and four types of rail materials (U71Mn, U75V, PG4 and PG5) were cross-matched to investigate the effects of bulk hardness, post-test hardness, hardening ratio, H_R/H_W on wear properties. The following main conclusions can be drawn:

1. The wheel and total wear rates decreased with the wheel bulk hardness, and slightly increased with the rail bulk hardness. However, the rail wear rates of the four rail materials decreased with the increase in the wheel bulk hardness under 1% creepage and 1500 MPa contact pressure. Notably, wear rates for the wheel-rail pairs with C-class and D-class wheels were substantially lower than those for other wheel-rail pairs.
2. The post-test surface hardness increased to a centralized range, 770 $HV_{0.5}$ ~ 870 $HV_{0.5}$ for wheels and 700 $HV_{0.5}$ ~ 900 $HV_{0.5}$ for rails. The wear rates of wheel, rail and total system were independent of wheel and rail post-test surface hardness.
3. The wheel and rail hardening ratios were dictated by the material properties, and decreased with their bulk hardness. Overall, the wear rates of wheel, rail and total system increased linearly with the increase in wheel hardening ratio, whereas, they were independent of rail hardening ratio.
4. In a wide pre-test H_R/H_W of 0.7 ~ 1.6, the wear rates of wheel, rail and total system generally increased with the increase in the pre-test H_R/H_W. The post-test H_R/H_W across

all experiments shifted to centralize in a range of 0.8 ~ 1.2, which made the effect of post-test H_R/H_W on the wear response not obvious.

5. The surface damage of high-hardness C-class and D-class wheels, and PG4 and PG5 rails was relatively slight. There was no significant difference in crack length of the five wheel steels. The fatigue cracks of premium PG4 and PG5 rails were significantly shorter cracks than those of the base materials (ER8-U71Mn), whereas, cracks of U75V were relatively longer.

Supplementary material

See supplementary material for Table S1, S2 and Figs. S1-S5.

Acknowledgements

The work was supported by National Natural Science Foundation of China (No.51975489), Fundamental Research Funds for the Central Universities (No.2682020CX29), Autonomous Research Project of State Key Laboratory (No.2020TPL-T10), Doctoral Innovation Fund Program of Southwest Jiaotong University (No. D-CX201810) and Cultivation Program for the Excellent Doctoral Dissertation of Southwest Jiaotong University.

References

[1] Y. Zhu, W.J. Wang, R. Lewis, W. Yan, S.R. Lewis, H. Ding, A review on wear between railway wheels and rails under environmental conditions, J Tribol, 141 (2019) 120801.

[2] A. Bevan, J. Jaiswal, A. Smith, M. Ojeda Cabral, Judicious selection of available rail steels to reduce

life-cycle costs, Proceedings of the Institution of Mechanical Engineers, Part F: Journal of Rail and Rapid Transit, 234(3) (2020) 257-275.

[3] M. Burstow, Wheel/rail hardness and total “system” wear”, V/T SIC Report TSPR033-00027 Issue 2, (2014).

[4] M. Benson, Effect of differential hardness on wheel/rail wear: literature survey, BRR Report LR MT 006, (1993).

[5] P.J. Bolton, P. Clayton, Rolling-sliding wear damage in rail and tyre steels, Wear 93(2) (1984) 145-165.

[6] H. Muster, H. Schmedders, K. Wick, H. Pradier, Rail rolling contact fatigue. The performance of naturally hard and head-hardened rails in track, Wear 191 (1996) 54-64.

[7] J. Liu, W. Jiang, S. Chen, Q. Liu, Effects of rail materials and axle loads on the wear behavior of wheel/rail steels, Advances in Mechanical Engineering 8(7) (2016) 1687814016657254.

[8] D. Markov, Laboratory tests for wear and rail and wheel steels, Wear 181-183 (1995) pp678-686.

[9] Y. Hu, L. Zhou, H.H. Ding, G.X. Tan, R. Lewis, Q.Y. Liu, J. Guo, W.J. Wang, Investigation on wear and rolling contact fatigue of wheel-rail materials under various wheel/rail hardness ratio and creepage conditions, Tribology International 143 (2020) 106091.

[10] J.W. Seo, S.J. Kwon, H.K. Jun, C.W. Lee, Effects of Wheel Materials on Wear and Fatigue Damage Behaviors of Wheels/Rails, Tribology Transactions 62(4) (2019) 635-649.

[11] R. Lewis, P. Christoforou, W.J. Wang, A. Beagles, M. Burstow, S.R. Lewis, Investigation of the influence of rail hardness on the wear of rail and wheel materials under dry conditions (ICRI Wear Mapping Project), Wear 430-431 (2019) 383-392.

[12] R. Stock, D. Eadie, K. Oldknow, Rail grade selection and friction management: a combined approach for optimising rail-wheel contact, Ironmaking & Steelmaking 40 (2013) 108-114.

[13] G. Vasic, Modelling of wear and crack initiation in rails, PhD Thesis, University of Newcastle Upon Tyne, 2013.

[14] I.J. McEwan, A review of laboratory-based wheel on rail wear studies carried out by the vehicle track interaction unit, BRR Report TR VTI 003, (1986).

[15] R. Heyder, K. Maedler, The influence of wheel and rail material on the wear of the respective contact partner, Proceedings of CM2015 10th International Conference on Contact Mechanics and Wear of Rail/Wheel Systems, Colorado, USA, 30 August-3 September 2015, 2015.

[16] R. Steele, R. Reiff, Rail-It's behaviour and relationship to total system wear, Proceedings of 2nd Conference on Heavy Haul. Colorado Springs, USA, 1982.

[17] X.J. Zhao, J. Guo, H.Y. Wang, Z.F. Wen, Q.Y. Liu, G.T. Zhao, W.J. Wang, Effects of decarburization on the wear resistance and damage mechanisms of rail steels subject to contact fatigue, Wear364-365 (2016) 130-143.

[18] H.H. Ding, C.G. He, L. Ma, J. Guo, Q.Y. Liu, W.J. Wang, Wear mapping and transitions in wheel and rail material under different contact pressure and sliding velocity conditions, Wear 352-353 (2016) 1-8.

[19] L. Ma, C.G. He, X.J. Zhao, J. Guo, Y. Zhu, W.J. Wang, Q.Y. Liu, X.S. Jin, Study on wear and rolling contact fatigue behaviours of wheel-rail materials under different slip ratio conditions, Wear 366-367 (2016) 13-26.

[20] J.P. Liu, Y.Q. Li, Q.Y. Zhou, Y.H. Zhang, Y. Hu, L. B. Shi, C.H. Tian, New insight into the dry rolling-sliding wear mechanism of carbide-free bainitic and pearlitic steel, Wear 432 (2019) 202943.

[21] K.M. Lee, A.A. Polycarpou, Wear of conventional pearlitic and improved bainitic rail steels, Wear 259(1-6) (2005) 391-399.

[22] R. Stock, R. Pippan, RCF and wear in theory and practice-the influence of rail grade on wear and RCF,

Wear 271(1-2) (2011) 125-133.

[23] P. Christoforou, D.I. Fletcher, R. Lewis, Benchmarking of premium rail material wear, Wear 436-437 (2019) 202990.

[24] Y. Hu, L. Zhou, H. H. Ding, R. Lewis, Q.Y. Liu, J. Guo, W.J. Wang. Microstructure evolution of railway pearlitic wheel steels under rolling-sliding contact loading. Tribology International 154 (2021) 106685.

[25] Y. Hu, L.C. Guo, M. Maiorino, J.P. Liu, H.H. Ding, R. Lewis, E. Meli, A. Rindi, Q.Y. Liu, W.J. Wang, Comparison of wear and rolling contact fatigue behaviours of bainitic and pearlitic rails under various rolling-sliding conditions, Wear 460-461 (2020) 203455.

[26] X. Hu, P. Van Houtte, M. Liebeherr, A. Walentek, M. Seefeldt, H. Vandekinderen, Modeling work hardening of pearlitic steels by phenomenological and Taylor-type micromechanical models, Acta Materialia 54 (2006) 1029-1040.

[27] Y.P. Wang, P.C. Xiang, H.H. Ding, W.J. Wang, Q. Zou, X.H. Liu, J. Guo, Q.Y. Liu, Effects of molybdenum addition on rolling contact fatigue of locomotive wheels under rolling-sliding condition, Materials 13 (2020) 4282.

[28] X. Cao, L.B. Shi, Z.B. Cai, Q.Y. Liu, Z.R. Zhou, W.J. Wang, Investigation on the microstructure and damage characteristics of wheel and rail materials subject to laser dispersed quenching, Applied Surface Science, 450 (2018) 468-483.

[29] R. Lewis, E. Magel, WJ Wang, U. Olofsson, S. Lewis, T. Slatter, A. Beagles, Towards a standard approach for the wear testing of wheel and rail materials. Proceedings of the Institution of Mechanical Engineers, Part F: Journal of Rail and Rapid Transit, 231(7) (2017) 760-774.

[30] W.R. Tyfour, J.H. Beynon, A. Kapoor, The steady state wear behaviour of pearlitic rail steel under dry rolling-sliding contact conditions, Wear 180 (1995) 79-89.

[31] M. Ueda, K. Matsuda, Effects of carbon content and hardness on rolling contact fatigue resistance in heavily loaded pearlitic rail steels, Wear 444-445 (2020) 203120.

[32] E. Sheinman, Wear of rails. A review of the American press, Journal of Friction and Wear 33(4) (2012) 308-314.

[33] J.F. Santa, P. Cuervo, P. Christoforou, M. Harmon, A. Beagles, A. Toro, R. Lewis, Twin disc assessment of wear regime transitions and rolling contact fatigue in R400HT-E8 pairs, Wear 432-433 (2019) 102916.

[34] J. Ding, I.R. McColl, S.B. Leen, P.H. Shipway, A finite element based approach to simulating the effects of debris on fretting wear, Wear 263 (2007) 481-491.

[35] L. Zhou, W.J. Wang, Y. Hu, S. Marconi, E. Meli, H.H. Ding, A. Rindi, Study on the wear and damage behaviors of hypereutectoid rail steel in low temperature environment, Wear (2020) 203365.

[36] A. Kapoor, F.J. Franklin, S.K. Wong, M. Ishida, Surface roughness and plastic flow in rail wheel contact, Wear 253(1-2) (2002) 257-264.

[37] W.T. Zhu, L.C. Guo, L.B. Shi, Z.B. Cai, Q.L. Li, Q.Y. Liu, W.J. Wang, Wear and damage transitions of two kinds of wheel materials in the rolling-sliding contact, Wear 398-399 (2018) 79-89.

[38] W.J. Wang, R. Lewis, B. Yang, L.C. Guo, Q.Y. Liu, M.H. Zhu. Wear and damage transitions of wheel and rail materials under various contact conditions. Wear, 362-363 (2016): 146-152.

[39] A.A. Razhkovskiy, T.G. Bunkova, A.G. Petrakova, O.V. Gateluk, Optimization of hardness ratio in rail-wheel friction pair, Journal of Friction and Wear 36(4) (2015) 334-341.